

1. Abstract and motivation

The generalized multi-pomeron exchange model [1] - [5] is proposed for the production in high energy heavy-ion collisions of hadrons containing heavy quarks. The main feature of this approach is the effective consideration of collectivity on the base of quark-gluon string fusion concept that provides the formation of new types of particle emitting sources – strings with higher tension. An increase in the string tension, in a certain class of events in pp and $A-A$ collisions characterized by high multiplicity of charged particles, allows to increase, in the process of string fragmentation, the creation of particles containing strange or charm quarks. The model parameters were defined in the previous analysis of data on the multiplicity dependence of the mean transverse momentum of charged particles in pp collisions over a wide energy range (from ISR to LHC). The yields of strange, multi-strange and charm particles are obtained as a function of multiplicity for pp and $Pb-Pb$ collisions at the LHC energy and compared with the experimental data.

2. Model

In this paper we present the application to the heavy ion collisions of the multi-pomeron model [1-4], initially developed for pp , $p\bar{p}$ interaction and then extended to the case of p - Pb [5]. According to the Regge-Gribov multi-pomeron exchange approach, in one nucleon-nucleon collision several pomeron exchanges can occur. Each pomeron exchange corresponds to a pair of quark-gluon strings, in the process of fragmentation of which the observed charged particles are produced. The multiplicity of charged particles can be obtained as:

$$N_{ch} = 2kn, \quad (1)$$

where k is the proportionality coefficient, n – number of pomerons.

We use equation (1) also in $A-A$ collisions case for the determination of mean number of pomerons $\langle n \rangle$ in each centrality class defined by the experimental data for multiplicity. According to the modified Schwinger mechanism [6, 1] in case of exchange of n pomerons the probability of the production of a primary hadron of the type ν with transverse momentum p_t is proportional to the value

$$\exp\left(-\frac{\pi(p_t^2 + m_\nu^2)}{t_{eff}}\right),$$

where m_ν is a mass of the particle, t_{eff} is the effective string tension. In the case of pp and p - Pb collisions:

$$t_{eff} = n^\beta t \quad (2)$$

where t is tension of a single string, and β is the parameter, responsible for the collectivity. Thus in $n^\beta t$ it takes into account the increase of string tension due to the string fusion mechanism [7]. The behaviour of parameter β as a function of the collision energy was defined from the data on $\langle p_t \rangle_{N_{ch}} - N_{ch}$ correlations in pp and $p\bar{p}$ collisions.

The value of parameter $\beta = 0$ means no collectivity, and no correlation between transverse momentum and multiplicity. At $\beta > 0$ ($\beta < 0$) the positive (negative) $\langle p_t \rangle_{N_{ch}} - N_{ch}$ correlation appears. The procedure for fixing the parameters is in detail described in the [2, 3]. In Fig. 1 an example at 7 TeV has shown, and also a model prediction at the top LHC energy, compared with the experimental data.

The values of the parameters were taken from the energy dependence of the parameters of the model as is [2, 3]:

$$k = 0.25 + 0.065 \ln \sqrt{s}, \quad \beta = 1.16 \left[1 - (\ln \sqrt{s} - 2.52)^{-0.19} \right], \\ t = 0.566 \text{ GeV}^2.$$

For $A-A$ case we substitute

$$t_{eff} = t \left(n \cdot \frac{S_0}{S(b)} \right)^\beta,$$

because in the string fusion approach [7] the string density, not a string number, matters. Here $S(b)$, the nucleus overlapping area, depends on impact parameter (b):

$$S(b) = R_0^2 (2\xi - \sin(2\xi)), \quad \xi = \arccos\left(\frac{b}{2R_0}\right), \quad (3)$$

and R_0 – radius of the nucleus (for Pb $R_0 = 7.276$ fm). For S_0 , the characteristic overlapping area in pp collisions we took inelastic nucleon-nucleon cross section ($S_0 = 6 \text{ fm}^2$). The resulting dependence of t_{eff} on multiplicity of Pb - Pb collisions is shown in Fig. 2.

The final hadron spectrum of strings fragmentation is modified due to the cascade decays of resonances. These decays are effectively taken into account by a cascade branching matrix $M_{\mu\nu}$, extracted from the particle decayer built into THERMINATOR 2 Monte Carlo generator [8]. For strangeness and multi-strangeness production for each particle we applied dedicated matrix in which the particle in question doesn't decay.

Finally, the relative yields of particles with the account of decays of hadrons have the form:

$$Y_\nu \sim \sum_\mu M_{\mu\nu} \cdot (2S_\mu + 1) \cdot \exp\left(-\frac{\pi(p_t^2 + m_\mu^2)}{t_{eff}}\right),$$

where S_μ is spin of a particle of the type μ , $M_{\mu\nu}$ is effective branching matrix. The yields of particles are normalized keeping the total multiplicity N_{ch} .

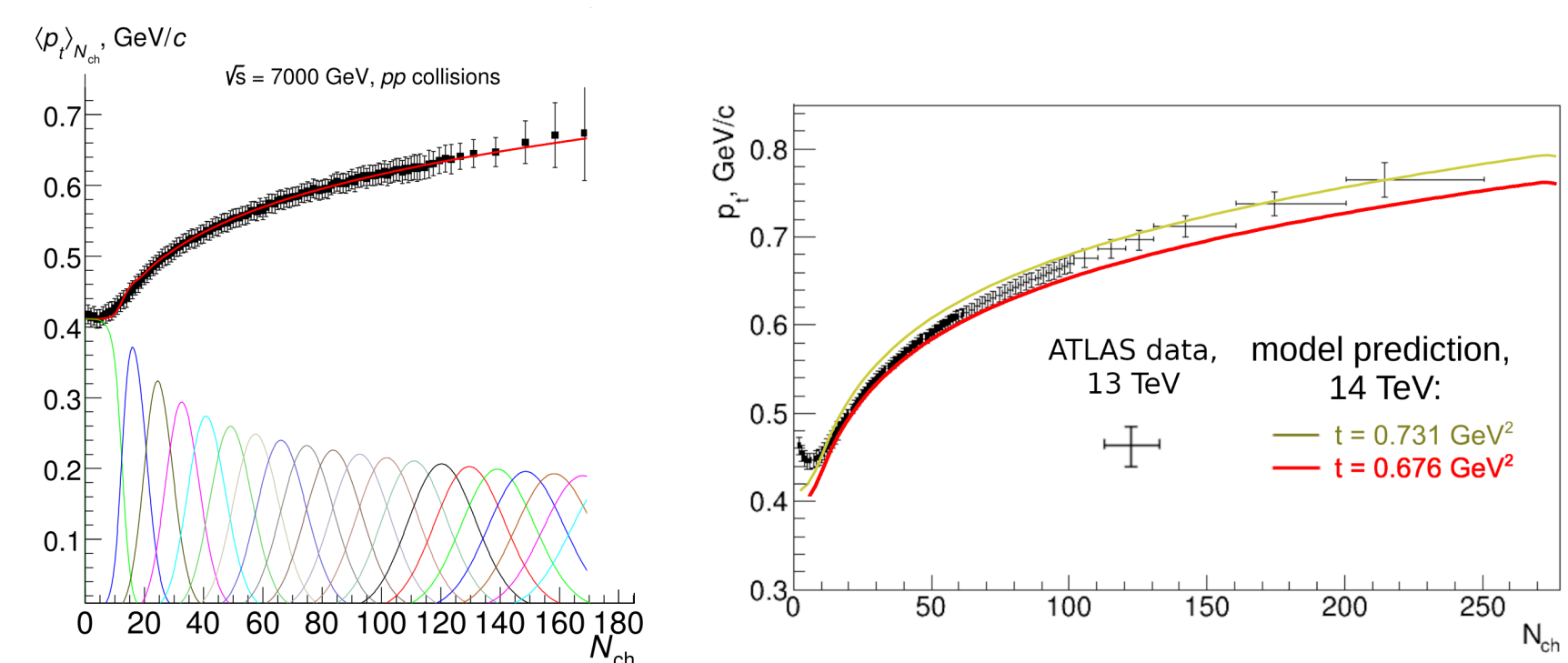


Figure 1: Left: example of previously performed fitting with a single parameter β of the multiplicity dependence of p_t in pp collisions at 7 TeV, showing contributions from different exchange of several soft pomerons [3] (experimental data from [9]). Right: prediction [2], obtained for 14 TeV, compared to experimental data at 13 TeV [10].

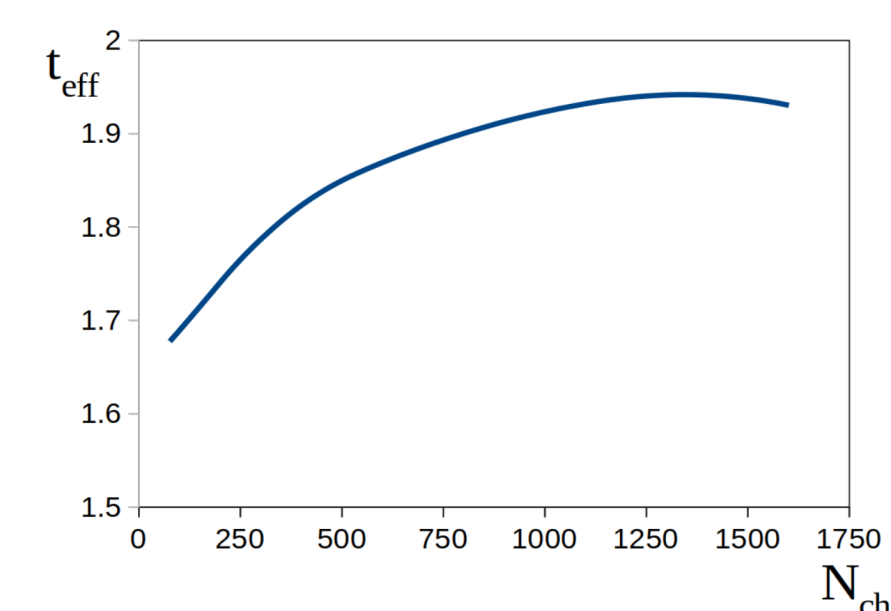


Figure 2: Multiplicity dependence of t_{eff} in $Pb-Pb$ collisions at $\sqrt{s}=2.76$ TeV.

3. Results

3.1 Energy dependence of the particle yields in pp collisions

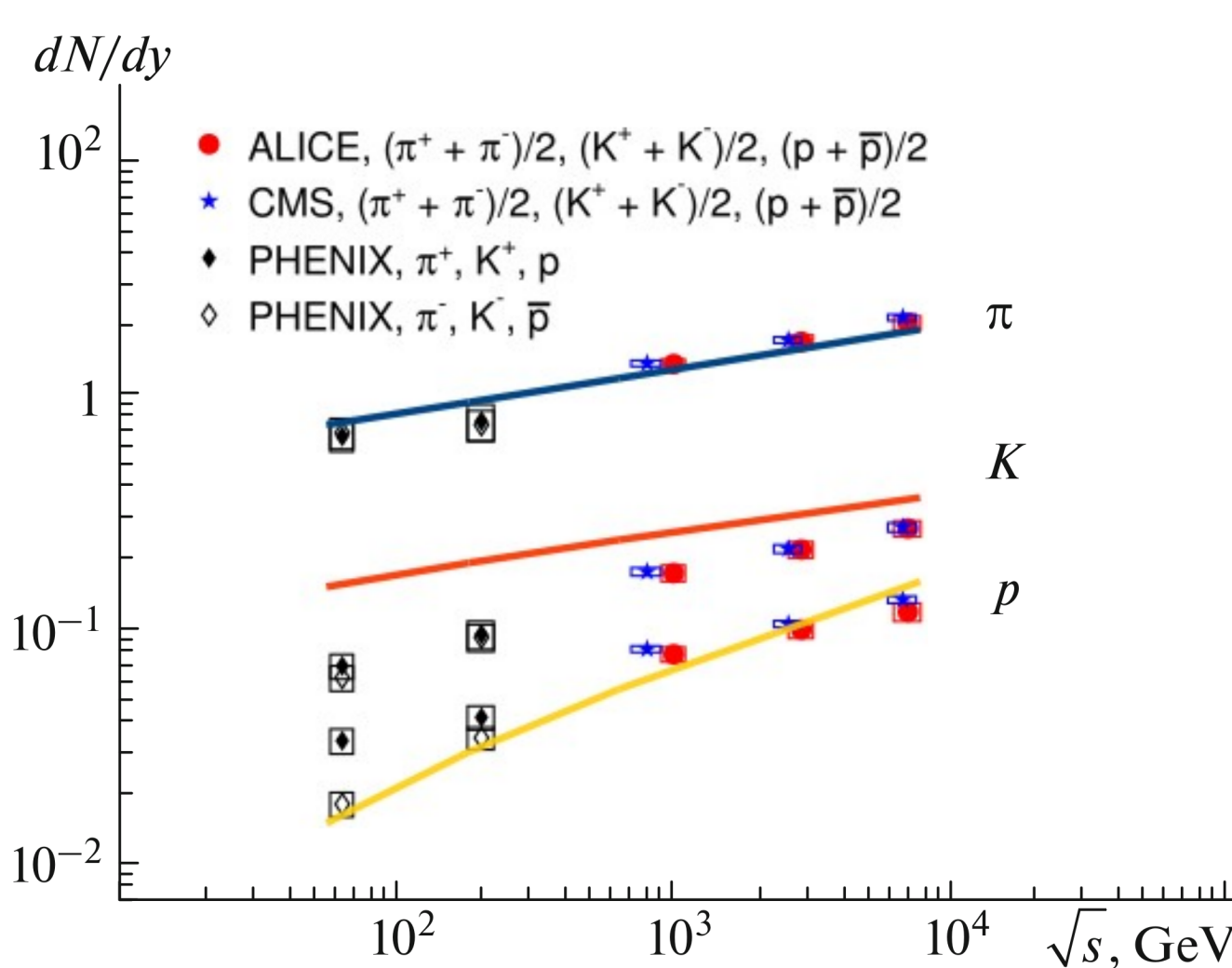


Figure 3: Energy dependence of the mean multiplicity per rapidity for charged pions, kaons, and protons in pp collisions [4,5]. The lines correspond to model calculations. The points denote experimental data (see references in [11]).

- The model demonstrates satisfactory agreement with experiment, which improves with energy.
- Discrepancies at lower energy could be related to the absence of the treatment of non-zero baryon density.

3.2 Multiplicity dependence of strangeness and multi-strangeness production

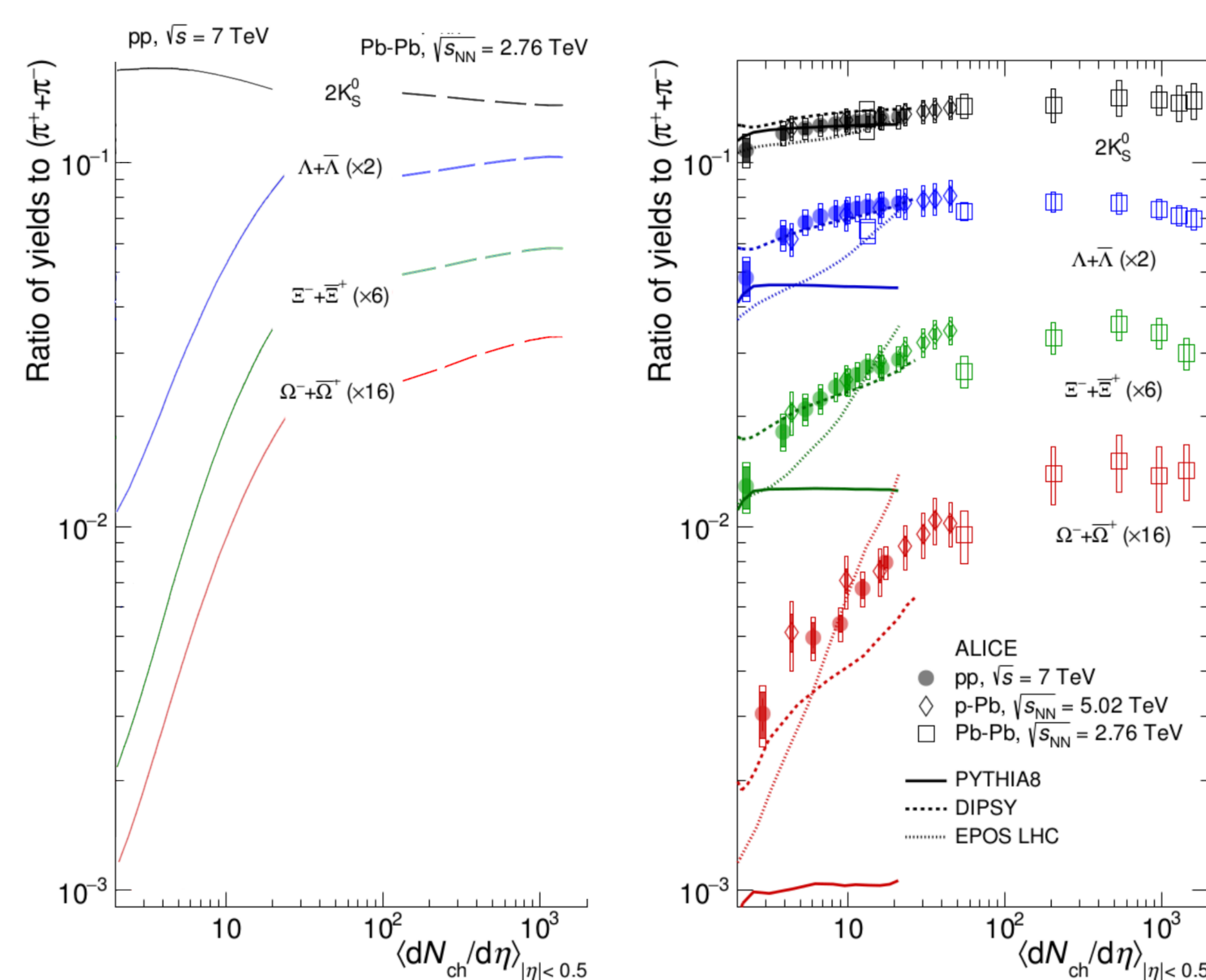


Figure 4: Multiplicity dependence of the strange and multi-strange particle yields ($K_s^0, \Lambda, \Xi, \Omega$) divided by charged pion multiplicity. Left plot – our model calculation for pp -collisions at $\sqrt{s} = 7$ TeV [4, 5] (solid lines) and for $Pb-Pb$ collisions (dashed lines) at $\sqrt{s_{NN}} = 2.76$ TeV (this work), right plot [12] – experimental data (dots) and prediction of other models.

- The model qualitatively describes the fast increase with charged particle multiplicity of the strangeness and multi-strange yields in pp collisions.
- The slope of the growth is even higher in the model than in the experimental data. This could be related to the fact that parameter β effectively considers all mechanisms for the transverse momentum growth, not only modification the string tension.
- The trend of the saturation and smooth transition from the pp to $Pb-Pb$ collisions is observed, similarly to the experimental data.

3.3 Open charm relative yield as the function of the multiplicity in pp and $Pb-Pb$ collisions

In this section we calculated the relative yield of D mesons in pp and $Pb-Pb$ collisions as a function of multiplicity.

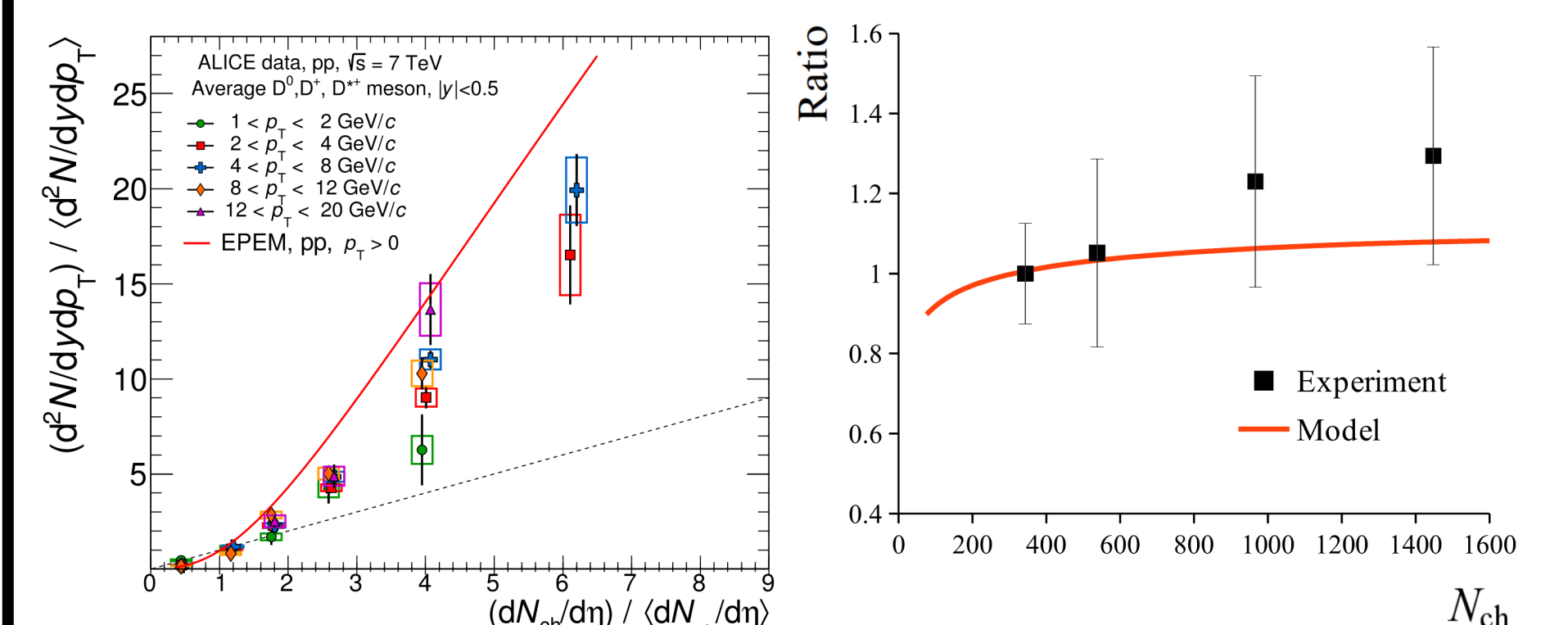


Figure 5: Left: The relative open charm yield in pp collisions at $\sqrt{s}=7$ TeV as a function of normalized charged multiplicity, calculated in model [5], compared with the experimental data [13]. The dotted line shows linear dependence of the yield (proportional to the total charged multiplicity). Right: Multiplicity dependence of D_0 meson production divided by pion multiplicity in $Pb-Pb$ collisions at 2.76 TeV, self-normalized in the 30-50% centrality class. The line shows model calculation, the dots – experimental data, which were extracted from the data of papers [14, 15]

- The model describes the slow growth of the relative D meson yield with multiplicity in $Pb-Pb$ collisions.
- This results confirm that production of open charm behaves very much similarly to that of pions, which has been observed in the experimental data, for example, on nucleon modification factors, or azimuthal flow.

4. Conclusions and outlook

The generalization of the multi-pomeron exchange model to nucleus-nucleus collisions is performed, taking into account the increase of strange and multi-strange particles and heavy flavour yield in the high string density overlap area of the colliding nuclei. The main feature of this model is the effective consideration of string collectivity (in a form of fusion) with the help of the dedicated parameter.

The model demonstrates a qualitative agreement with the experimental data on the correlation of the strange baryons and charmed meson yields with the charged particles multiplicity.

The D-meson relative yield has been calculated in $Pb-Pb$ collisions at 2.76 TeV and compared with the available experimental data. A slow growth of D-meson relative yield with multiplicity in $Pb-Pb$ collisions is also described by the generalized multi-pomeron exchange model.

The future studies would include a more accurate accounting of Schwinger mechanism (on the quark level), statistical fragmentation models application, and also calculation of different correlations in our framework.

References

- [1] N. Armesto, D. Derkach, and G. Feofilov // Phys. Atom. Nucl. 2008, V. 71, P. 2087.
- [2] E. Bodnia, D. Derkach, G. Feofilov, V. Kovalenko, A. Puchkov // PoS (QFTHEP 2013) 060 (2013), arXiv:1310.1627 [hep-ph].
- [3] E. O. Bodnia, V. N. Kovalenko, A. M. Puchkov, G. A. Feofilov // AIP Conf. Proc. 2014, V. 1606, P. 273-282, arXiv:1401.7534 [hep-ph].
- [4] Feofilov G., Kovalenko V., Puchkov A. // arXiv:1710.08895 [hep-ph]. 2017.
- [5] Feofilov G., Kovalenko V., Puchkov A. // EPJ Web of Conferences. 2018. Vol. 171, P. 18003, arXiv:1711.00842 [nucl-th].
- [6] J. Schwinger // Phys. Rev. 1951. V. 82, P. 664; T. S. Biro, H. B. Nielsen, and J. Knoll // Nucl. Phys. B. 1984, V. 245, P. 449.
- [7] M. A. Braun, C. Pajares // Nucl. Phys. B. 1998. V. 390. P. 542.
- [8] M. Chojnacki, et al // Comput. Phys. Commun. 2012. V. 183. P. 746-773. arXiv:1102.0273 [nucl-th].
- [9] V. Khachatryan, et al. (CMS Collaboration) // JHEP. 2011. V. 1101. P. 079.
- [10] M. Aaboud, et al. (ATLAS Collaboration) // Eur. Phys. J. C. 2016. V. 76. P. 502.
- [11] J. Adam et al. (ALICE Collaboration) // Eur. Phys. J. C. 2015. V. 75. P. 226.
- [12] J. Adam, et al (ALICE Collaboration) // Nature Physics. 2017. V. 13. P. 535-539.
- [13] J. Adam, et al. (ALICE Collaboration) // JHEP. 2015. V. 09, 148, arXiv:1505.00664 [nucl-ex].
- [14] J. Adam et al. (ALICE Collaboration) // JHEP. 2015. V. 1511. P. 205; 2017. JHEP V. 1706. P. 032.
- [15] B. Abelev et al. (ALICE Collaboration) // JHEP. 2012. V. 1209. P. 112.